Application Note

# Hall Effect for Sensing and Materials Characterization

Zurich Instruments

Applications: Quantum and Nano Electronics, Low-Temperature Physics, Transport Measurements
Products: MFLI, MF-MD

Release date: August 2018

## Introduction

Since the discovery of the Hall effect in 1879 by Edwin Hall, it has been widely applied in measurements, particularly in materials characterization and sensing. Today it is being used to characterize new materials, enabling the discovery of new phenomena, such as the quantum Hall effect, spin Hall effect and, more recently, topological insulators [1]. The Hall effect also serves as a platform for many device applications, such as current sensing in the automotive industry, metrology, non-destructive inspection and testing, and security screening applications.

The Hall effect appears when a conductor is placed in a magnetic field B, as shown in Figure 1. The charge carriers flowing through the conductor are deflected due to the Lorentz force $F_L$ causing a transverse, or Hall voltage $V_{xy}$, between the sides of the material, perpendicular to both the magnetic field and the current $I_R$. The Hall voltage is linearly proportional to the magnetic field, while the longitudinal voltage $V_{xx}$ is magnetic field independent. These are the classical Hall effect signatures for metallic conductors and semiconductors, as illustrated in Figure 2 (a). The resistivity $\rho$ of a bulk conductor is defined as $\rho = R w t / l$, where $R = V/I$ is the resistance, w is the width, t is the thickness, and l is the length of the conductor. The resistivities $\rho_{xx}$ and $\rho_{xy}$ are derived from the classical Drude model in the form:

$$\rho_{xy} = \frac{B}{n e t} \qquad (1a)$$

$$\rho_{xx} = \frac{m}{n e^2 \tau} \qquad (1b)$$

where n is the density of charge carriers, m is the carrier effective mass, e is the electron charge, and $\tau$ is the mean free scattering time [2]. Equation 1a describes the transverse Hall resistivity with a linear magnetic field and inverse carrier density dependence, whereas Equation 1b describes the longitudinal resistivity which is field independent and reflects the transport characteristics of the material in the direction of current. Two main applications of the classical Hall effect are:

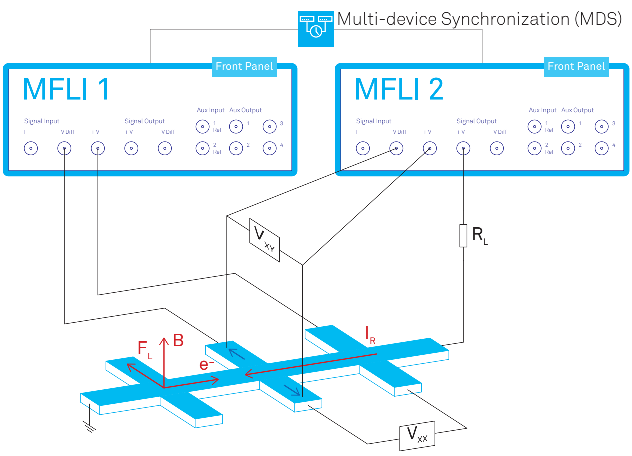


**Figure 1.** Schematic showing the Hall effect measurement setup in a standard Hall bar geometry. Two lock-in amplifiers are used to measure the voltages $V_{xx}$ and $V_{xy}$ along and perpendicular to the current flow. The conventional current $I_R$ flow direction is used in the diagram, so that the motion of electrons is in the opposite direction. The Lorenz force $F_L$ is perpendicular to the magnetic field B and the charge carrier motion.

### 1. Materials characterization

A material's conducting properties are determined using Hall effect measurements. From the Hall resistivity, the carrier concentration n and carrier type are determined using Equation 1a because the magnetic field dependence is linear. Longitudinal resistivity measurements are used with Equation 1b to determine conductivity $\sigma_{xx} = 1/\rho_{xx}$ and carrier mobility $\mu = \sigma_{xx}/n\,e$. The Hall bar geometry (as shown in Figure 1) was designed to extract the voltages $V_{xx}$ and $V_{xy}$ as well as the current $I_R$ directly.

### 2. Sensing

When the conducting properties of a material are known, the Hall voltage and its linear proportionality to the perpendicular magnetic field component can be used to build sensitive and accurate magnetic field sensors. In this case, the measured voltage is proportional to the magnetic field and can be extracted from Equation 1a. As the linearity spans from zero to fields of several Tesla (T), Hall sensors are widely used in industrial applications as Hall probes, speedometers, Hall switches, proximity and current sensors. In many of these applications the measurement speed is also important, while the signals are often on top of another large signal and noise background coming from various static and time varying field noise sources. This sets demanding requirements for the measurement electronics.

AC measurement techniques are particularly well suited for such requirements as they help to avoid certain systematic measurement errors, such as thermal offsets, thermal drift, and unwanted components in the background noise spectrum. In addition, a higher signal-to-noise ratio (SNR) is achieved compared to DC techniques, primarily because the background noise falls as 1/f with increasing frequency f. Higher SNR usually also leads to faster measurements. In addition, AC techniques often come with higher measurement resolution, enabling a larger dynamic range.

## Lock-In Amplifiers for Accurate and Fast Measurements

AC measurements are best performed with lock-in amplifiers, as they measure reliably down to a few nV with adjustable bandwidth, even in the presence of significant background noise. These instruments use phase-sensitive detection to measure the amplitude of a signal and the phase against a reference frequency. Background noise at frequencies other than the reference frequency and outside the measurement bandwidth are heavily rejected and do not impact the measurement.

A typical setup using the Hall bar geometry and two Zurich Instruments MFLIs, 500 kHz lock-in amplifiers, is shown in Figure 1. The two lock-in amplifiers are used to measure the transverse Hall voltage $V_{xy}$ and longitudinal voltage $V_{xx}$, while one of them also provides the current through the sample over a so-called current limiting resistor $R_L$. This resistor is typically chosen to be much larger than any of the resistances combined in the circuit, so the current can be assumed constant. Materials characterization measurements are typically performed at frequencies up to a few tens of Hertz, with the two lock-in amplifiers synchronized in terms of measurement frequency and data sampling. The constant current assumption holds in many cases, but in studies where the sample impedance changes dramatically over the course of a measurement, the current needs to be carefully monitored. With its current sensing input, the MFLI has this capability. It measures the current at the same frequency as the voltage input. For a more detailed treatment of lock-in amplifiers and how they work see [3].

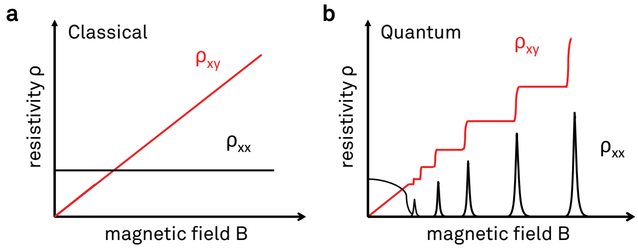


**Figure 2.** Illustration of longitudinal and transverse resistivities $\rho_{xx}$ and $\rho_{xy}$ plotted as a function of the magnetic field. (**a**) Classical Hall effect behavior, where $\rho_{xy}$ is co-linear with B, and $\rho_{xx}$ is independent of B. (**b**) Typical signatures of the integer quantum Hall effect. The Hall resistivity $\rho_{xy}$ shows plateaus for a range of magnetic field values, with $\rho_{xx}$ going to zero at the same time.

## Quantum Hall Effect in 2DEGs

When the electrons of a two-dimensional electron gas (2DEG) are placed in a magnetic field, the Hall effect exhibits qualitatively new features. The Hall resistivity changes in steps with plateau structures occurring as the magnetic field increases. At the same time, the longitudinal resistivity drops to zero. This is known as the quantum Hall Effect (QHE), a quantum mechanical phenomenon, where the discrete energy levels, the so called Landau levels, are formed in the density of states of a 2DEG. The typical behavior is shown in Figure 2 (b). While on a plateau, the electrons follow discrete circular orbits with quantized energy levels and travel macroscopic distances along the edges of a sample without any resistance. This is quite remarkable as the conduction is still carried by electrons and its dissipationless nature points to the topologically protected edge states. In addition, the electrons moving between the Landau levels can cause observable “quantum oscillations”, known as Shubnikov–de Haas (SdH) oscillations, see Figure 3. The integer QHE was discovered by Klaus von Klitzing in 1980 [4], winning him the Nobel prize in 1985.

The Hall resistivity for a specific plateau is given by:

$$\rho_{xy} = \frac{h}{\nu\, e^2}\,,\text{while} \quad \rho_{xx} = 0. \tag{2}$$

Here, $\nu$ is an integer called the filling factor and $h/e^2$

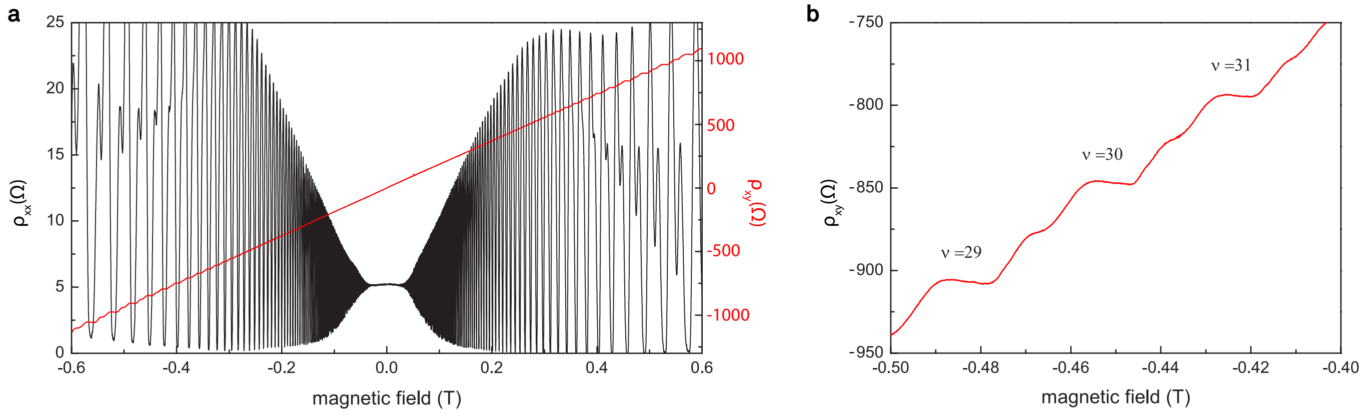


Figure 3. (a) Plot of longitudinal and transverse resistivity $\rho_{xx}$ and $\rho_{xy}$ as a function of the magnetic field B, using two lock-in amplifiers. Note that $\rho_{xy}$ changes sign when the field direction is inverted. (b) A zoom into the measurement data from (a) shows several higher order Hall plateaus at negative fields with the prominent signatures of spin splitting between them.

is a fundamental constant known as the von Klitzing constant equal to $R_K = 25812.807557(18)\,\Omega$ or the quantum of resistance. Note that the resistivity and resistance in 2DEGs have the same unit Ω since $\rho = R\,w/l$. The $R_K$ depends only on the Planck constant h and electron charge e and not on the material properties, temperature fluctuations, or crystal impurities. In addition to the QHE in a 2DEG, other types of Hall effect phenomena have been discovered. These include the fractional Hall effect, spin Hall effect, and recent studies have also shown a "quantum anomalous Hall effect", where thin films of topological insulators can exhibit a QHE at zero external magnetic field [5].

### Hall Effect Case Study

The QHE was measured using two MFLIs at the ETH Zurich where 2DEG $GaAs/Al_{0.3}Ga_{0.7}As$ samples were characterized for the purpose of a study of light-matter coupling [6]. The electron mobility μ was $3 \times 10^6\,cm^2/V\,s$ and the electron density n was $3 \times 10^{11}\,cm^{-2}$. The Hall bar dimensions were 166.5 μm long and 39 μm wide. An example of measurements shown in Figure 3 were performed at 100 mK and at a frequency of 14 Hz. A current of 20 nA was obtained by applying an RMS voltage of 200 mV across the 10 MΩ current limiting resistor, placed in series with a Hall bar. The signal was amplified by a home built preamplifier with a signal amplification of 1000 before the lock-in input. The lock-in measurements were done using a time constant of 100 ms.

Figure 3 (a) shows a plot of longitudinal and transverse resistivities $\rho_{xx}$ and $\rho_{xy}$ as a function of the magnetic field B, obtained using two lock-in amplifiers. The black trace shows SdH oscillations in $\rho_{xx}$ and the integer quantum Hall effect plateaus in $\rho_{xy}$ are displayed in red. The first plateau is formed at about 13 T (not shown). In this measurement the filling factor of up to 300 was observed, with the early onset of SdH oscillations as a result of the low temperatures and the high mobility of the sample, reflecting its high quality. Also, structures in $\rho_{xx}$ forming above 0.4 T are due to spin splitting of the Landau levels (see Figure 3 (b)).

### Practical uses of QHE and related phenomena

Due to the quantum Hall states' resistance being independent of material type, scattering and temperature, 2DEG materials are used as resistance standards. Until recently the QHE was observed only at low temperatures. In 2007, measurements on graphene at a magnetic field of 20 T revealed the QHE at room temperature [7], and the potential basis to develop new resistance standards. The discovery of the QHE in topological insulators without the presence of a magnetic field opened another set of new possibilities. These new materials that conduct in protected states could be used for fast electronics and quantum computation [1].

## Advantages of using the MFLI for Hall Effect Measurements

### 1. High sensitivity: extract the smallest signals

Hall effect measurements involve detection of small signals often buried in the noise. The typical resistance in Hall Effect Measurements is about 100 Ω or less. Combined with a current of about 20 nA, this converts into voltages of a few μV for $V_{xx}$ and hundreds of μV for $V_{xy}$. The use of a preamplifier is certainly beneficial in order to increase the SNR through amplification and filtering of the broadband noise. Both voltage measurements require the high dynamic range of the MFLI inputs to accommodate the full magnetic field sweep. This is also essential in order to resolve small features.

### 2. Effective noise rejection: maximize SNR

Effective noise rejection is crucial for achieving high SNR. The MFLI is equipped with 8 order filters capable of rejecting noise up to a million times bigger than the measured signal, providing enough margin to optimize for both measurement speed and accuracy. In addition, when measurements are carried out at low temperatures, the noise originating from the lock-in input affects sample's electronic temperature and adds to the overall noise. In this respect, the MFLI provides the best commercial solution on the market, as its inputs have the lowest power dissipation available [8]. The efficient noise rejection of the lock-in effectively speeds up the measurement since the filter time constants can be shortened and the full characterization measurement time in some cases lasts between a day or a week, can be reduced by up to a factor of 10.

#### 3. High accuracy: dedicated current sensing

In cases where the constant current $I_R$ assumption does not hold, it is important to measure the current $I_R$ to achieve highly accurate resistance measurements and avoid the systematic error of up to 10%. With the MF-MD option available, the current can be simultaneously measured with Hall voltage using just one lock-in amplifier unit. The user benefits from reduced setup complexity and increased measurement fidelity.

#### 4. Efficient work-flows: LabOne software included

LabOne, the Zurich Instruments control software provided with the MFLI, is designed for efficient workflows. The intuitive user interface takes the user quickly to first results, while a wealth of features and tools will help to gain high confidence in the acquired data. For instance, while data are directly recorded at the Signal Inputs with the Scope and the demodulator outputs can be visualized in the time (frequency) domain using the Plotter (Spectrum Analyzer).
If the measurements require the use of more than one instrument, the multi-device synchronization (MDS) feature will be valuable. MDS keeps the reference clocks of all instruments synchronized and the time stamps of the recorded data aligned. The measurements can still be carried out within a single session of the LabOne user interface.
In case measurements need to be automated or the MFLI being integrated into an existing measurement environment, LabOne provides APIs for LabVIEW®, MATLAB®, Python, .NET and C.

## Conclusion

Today, Hall effect measurements are ubiquitous in fundamental research, SI unit redefinition and industrial applications. Most of the measurements benefit from using AC techniques where lock-in amplifiers are the prime tool to guarantee high accuracy and SNR through optimum noise rejection.

The Zurich Instruments MFLI Lock-in Amplifier is built on the latest hardware and software technologies, combining the benefits of high performance digital signal processing with ease of use. From simple measurements detecting a Hall voltage at a defined frequency to more complicated setups requiring the use of multiple instruments, the MFLI is the right tool to use. It can adapt to changing requirements, for instance by upgrading the frequency range from DC to 500 kHz to DC to 5 MHz or adding another 3 demodulators to analyze the voltage and current inputs simultaneously.

Please contact us to discuss your Hall measurement requirements (info@zhist.com or +41 44 5150 410). For more information on the MFLI Lock-in Amplifier visit https://www.zhinst.com/products/mfli.


## Acknowledgements

We are grateful to Gian L. Paravicini-Bagliani from the Quantum Optoelectronics Group at ETH Zurich for sharing and discussing the Quantum Hall effect data with us.


## References


[1] Davide Castelvecchi. The strange topology that is reshaping physics. Nature, 547:272–274, 2017.

[2] N. W Ashcroft and N.D. Mermin. Solid state physics. 1976.

[3] Zurich Instruments AG. Principles of Lock-in Detection, 2017. White Paper.

[4] K. v. Klitzing, G. Dorda, and M. Pepper. New method for high-accuracy determination of the fine-structure constant based on quantized hall resistance. Phys. Rev. Lett., 45:494–497, Aug 1980.

[5] A. J Bestwick, E. J. Fox, X. Kou, L. Pan, K. L. Wang, and D. Goldhaber-Gordon. Precise quantization of the anomalous hall effect near zero magnetic field. Phys. Rev. Lett., 114:187201, May 2015.

[6] G. L. Paravicini-Bagliani, F. Appugliese, E. Richter, F. Valmorra, J. Keller, M. Beck, N. Bartolo, C. Rössler adn T. Ihn, K. Ensslin, C. Ciuti, G. Scalari, and J. Faist. Magneto-transport controlled by landau polariton states. arXiv:1805.00846, 2018.

[7] K. S. Novoselov, Z. Jiang, Y. Zhang, S. V. Morozov, H. L. Stormer, U. Zeitler, J. C. Maan, G. S. Boebinger, P. Kim, and A. K. Geim. Room-temperature quantum hall effect in graphene. Science, 315(5817):1379–1379, 2007.

[8] Zurich Instruments AG. Power Dissipation at Input Connectors of Lock-in Amplifiers, 2017. Technical Note.




Technoparkstrasse 1
CH-8005 Zurich
Switzerland

www.zhinst.com
info@zhinst.com
+41 44 515 04 10